

## Article

# Computerized Optical Impression Making of Fully Dentate Upper and Lower Jaws: An In Vitro Study

Lukas Droste <sup>1,\*</sup> , Kirstin Vach <sup>2</sup> , Ralf J. Kohal <sup>1</sup>  and Sebastian B. M. Patzelt <sup>1,3</sup> 

<sup>1</sup> Department of Prosthetic Dentistry, Medical Center—University of Freiburg, Faculty of Medicine, University of Freiburg, 79106 Freiburg, Germany; ralf.kohal@uniklinik-freiburg.de (R.J.K.); sebastian.patzelt@uniklinik-freiburg.de (S.B.M.P.)

<sup>2</sup> Institute for Medical Biometry and Statistics, Faculty of Medicine, University of Freiburg, 79104 Freiburg, Germany; kirstin.vach@uniklinik-freiburg.de

<sup>3</sup> Private Dental Clinic, Am Dorfplatz 3, 78658 Zimmern ob Rottweil, Germany

\* Correspondence: lukas.droste@mail.medizin.uni-freiburg.de

**Abstract:** Objectives: The aim of this experimental study was to evaluate the accuracy of five intraoral scanners for digitizing fully dentate unprepared maxillae and mandibulae in vitro. Materials and Methods: One maxillary and one mandibular reference model with acrylic teeth, an industrial grade reference scanner, 3D evaluation software and the intraoral scanners CS 3500, iTero HD2.9, Planmeca PlanScan, TRIOS Standard and 3M True Definition were used. Scans of the entire arches, one front and two side segments of each arch scan of maxilla and mandibula were evaluated separately for trueness and precision. In addition, visual analyses of deviation patterns, surface properties and approximal areas were performed with the aid of 3D evaluation software. Results: The intraoral scanners CS 3500, TRIOS Standard and iTero HD2.9 showed a similar level of trueness. The True Definition scanner showed lower full arch trueness compared to the TRIOS Standard and to the iTero HD2.9 ( $p < 0.05$ ). Full arch trueness of the PlanScan was lower compared to the other scanners. Video-based systems showed higher numbers of datapoints per scan (127,300–169,730) compared to single image-based systems (64,115–88,124). The acquisition of interproximal areas was insufficient across all scanners. Limitations: The intraoral scanners were not tested under clinical conditions in this study. Conclusions: Apart from interproximal areas, clinically acceptable full arch trueness was achieved by the CS 3500, the iTero HD2.9 and the TRIOS Standard.

**Keywords:** intraoral scanners; full arch scans; unprepared teeth; maxilla and mandibula; accuracy; deviation pattern; number of datapoints; tessellation; interproximal areas; aligners



**Citation:** Droste, L.; Vach, K.; Kohal, R.J.; Patzelt, S.B.M. Computerized Optical Impression Making of Fully Dentate Upper and Lower Jaws: An In Vitro Study. *Appl. Sci.* **2024**, *14*, 2370. <https://doi.org/10.3390/app14062370>

Academic Editor: Nir Shpack

Received: 12 February 2024

Revised: 4 March 2024

Accepted: 6 March 2024

Published: 12 March 2024



**Copyright:** © 2024 by the authors. Licensee MDPI, Basel, Switzerland. This article is an open access article distributed under the terms and conditions of the Creative Commons Attribution (CC BY) license (<https://creativecommons.org/licenses/by/4.0/>).

## 1. Introduction

Intraoral impressions are an important part of everyday work in dental medicine. They serve diagnostic, forensic and treatment purposes. Intraoral impressions can be subdivided into conventional physical impressions and into intraoral digital impressions. Conventional and digital impression systems are used to produce physical study models, physical working models and digital models that can be used for diagnostic purposes such as virtual articulation or direct appliance production [1–3].

Intraoral digitization, also called computerized optical impression making (COIM), seems to have become the new method of choice because it provides numerous advantages such as real-time visualization, easier repeatability, no need for cleaning of conventional impression trays, no cast pouring and no wear of the study or working model [4]. It reduces the number of steps needed to obtain a master cast compared to conventional methods. This direct way of impression making also offers benefits in time efficiency compared to conventional impression methods needed for laboratory scanning processes as well as improved patient comfort [5–7]. Apart from the fields of prosthodontics and implantology, computerized optical impression making is increasingly used in orthodontic treatments [8].

for example, for the customization and placement of brackets and for the production of temporary anchorage devices (TADs), clear aligners and retainers [9–17].

Nonetheless, to establish a fully digital workflow in clinical practice is challenging. It can include high costs for an intraoral scanner, associated hardware and software. COIM in daily practice usually requires an internet connection, which is not available in every orthodontic clinic. Furthermore, the use of intraoral scanners requires training, which can be particularly difficult for clinicians unfamiliar with operating digital technology [18]. Moreover, digitally measured tooth crowding can differ from conventionally measured crowding [19]. Intraoral scanners can provide different levels of accuracy, time efficiency as well as a variety of additional capabilities like automated caries detection. These features depend on the manufacturer, model generation and software version of the intraoral scanner [6,20–22], which leads to different indication spectrums of intraoral scanners. This further increases the complexity of integrating COIM into daily practice. In addition, the current literature shows that full arch scans are still challenging for intraoral scanners, with significantly decreased accuracy compared to partial arch scans [23].

As the first step along a digital clinical workflow, it is important to use an intraoral scanner which generates optical impressions with high accuracy because digital impressions with a low accuracy impair the accuracy of the digital model used for diagnostic purposes or for appliance design. An impression system was considered to yield the highest accuracy if it showed the lowest trueness and precision values and thus the highest trueness and precision compared to the other intraoral scanners tested in this study. The aim of the trueness evaluations was to determine 3D deviations between the reference datasets which were generated with the aid of an industrial scanner and the oral scanners' datasets. The term trueness is defined as the closeness of agreement between the average value obtained from a large series of test results and an accepted reference value. It relates to how close the measured size of the scanned teeth is to the real size of the teeth. The real size of the scanned teeth was anticipated with the aid of the industrial scanner. The aim of the precision comparisons was to determine the repeatability of the five intraoral scanners tested in this study. The term precision tells us to what extent the different measurement values of the same measurement system and the same object differ from each other [24].

## 2. Materials and Methods

### 2.1. Materials

For this *in vitro* investigation, acrylic models of the upper and lower jaw were used (Figure 1). These models consisted of 28 acrylic teeth (Simple Root Tooth Model [A5A-200], Nissin Dental Products, Kyoto, Japan) and a self-curing acrylic denture material (Instant Tray Mix Liquid/Self Curing Denture Liquid [#0856FIB] Lang Dental, Wheeling, IL, USA).

The reference scanner used for the trueness comparisons was an industrial grade optical stereo camera measuring system (ATOS III Triple Scan, GOM, Braunschweig, Germany). The five intraoral scanners evaluated in this study (Table 1) used different software: The CS 3500 (CS) was equipped with Dental Imaging Software (version 6.13.3) and firmware (version 1.1.10.0). The scanning process was performed with the CS Acquisition Interface (product version 1.1 and internal version 1.1.4) with the acquisition type "Orthodontics". The iTero HD2.9 (IT) was equipped with software (version number 5.1.1.158). The Planmeca PlanScan (PS) was equipped with the internal scanner software (version 3.5.1.12) and the Romexis CAD-Module (version 5.2.0.11, Planmeca/E4D Technologies, Richardson, TX, USA). The TRIOS Standard dental scanner (TR) was equipped with firmware (version number 4|0|0302) and software (version number 1.2.1.4). The 3M True Definition (TD) was operated with scanning software (version number 4.2.1). The latter scanner, in contrast to the former scanners, required a titanium oxide reflective powder (High Resolution Scanning Spray, 3M ESPE Dental Products, Saint Paul, MN, USA) to powder the artificial teeth. Three-dimensional evaluation software (Geomagic Control; version 2014.3.0.1781, 3D Systems, Rock Hill, SC, USA) was used for the 3D analyses.



**Figure 1.** Maxillary and mandibular reference models.

**Table 1.** Specifications of the intraoral scanners.

Scanner	Manufacturer	Data Capture Principle	Data Capture Mode
CS 3500 (CS)	Carestream Health, Rochester, MN, USA	Triangulation	Individual images
iTero HD2.9 (IT)	Align Technology, San José, CA, USA	Parallel confocal imaging	Individual images
Planmeca PlanScan (PS)	Planmeca/E4D Technologies, Richardson, TX, USA	Triangulation	Video sequence
TRIOS Standard (TR)	3Shape, Copenhagen, Denmark	Confocal microscopy	Video sequence
3M True Definition (TD)	3M ESPE, St. Paul, MN, USA	Wavefront sampling	Video sequence

## 2.2. Methods

All scans were conducted at an average room temperature of  $22.1 \pm 0.89$  °C, an average relative air humidity of  $43.8 \pm 24.8\%$  and clinical ambient light conditions. First, the maxillary and mandibular reference models were scanned with the reference scanner (ATOS III Triple Scan). Afterwards, the reference models were scanned three times with the TR, PS, IT, CS and lastly with the TD which required powder coating. If available, the scans were performed according to the manufacturers' instructions. In case these instructions were not available, the best-known scan strategy was used (Figure 2).

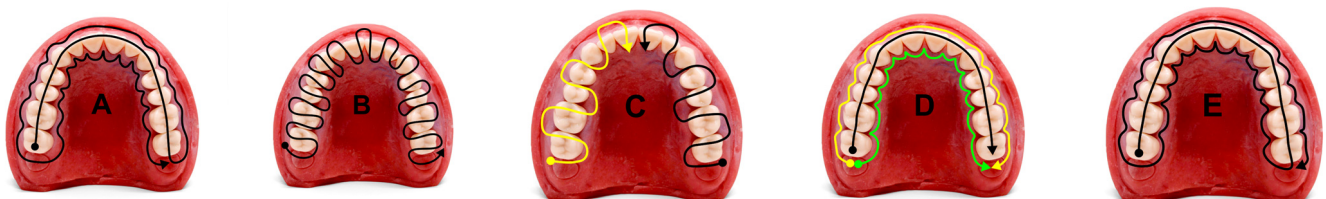


**Figure 2.** Maxillary and mandibular scanning protocols for the complete arch scans. Dots indicate the start of the scanning paths while the arrows indicate the end of the scanning paths: (A) TR, (B) PS and (C) IT: First, the area indicated with the black arrow was scanned with subsequent scanning of the area marked with the yellow arrow. (D) CS: First, the occlusal area indicated with the black arrow was scanned. Second, the buccal areas (yellow) were scanned with subsequent scanning of the lingual areas marked with the green arrow. (E) TD.

Afterwards, the scan files were imported into the 3D evaluation software (Geomagic Control), and areas of the generated scan files which did not belong to the surface of the

teeth were removed. In addition, four different datasets out of one complete dental arch scan file were generated: One full dental arch dataset; two side segment datasets, which are composed of the premolars and molars; and one front segment dataset, which is composed of the canines and incisors (Figures 3 and 4).

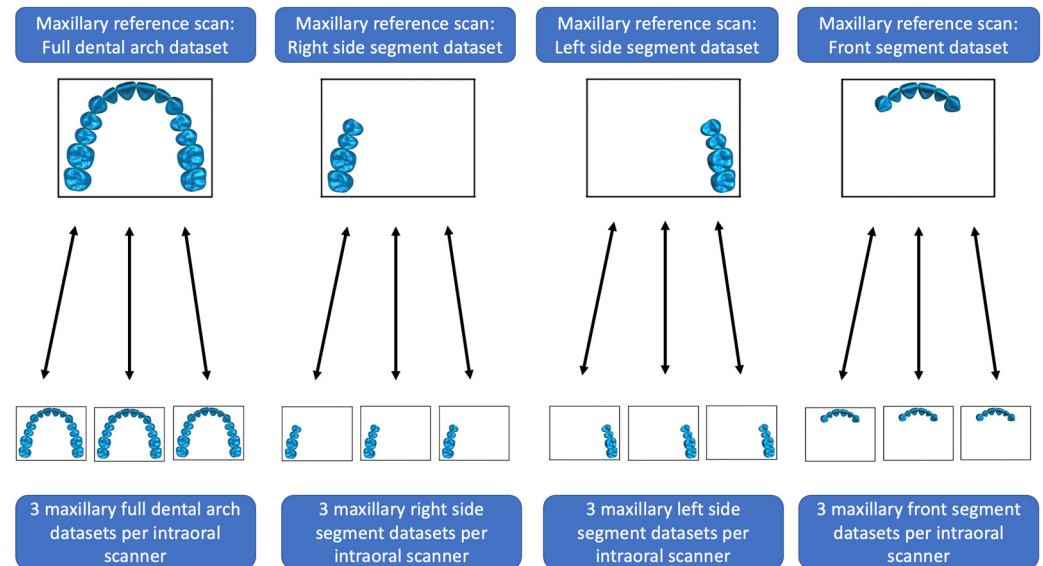


**Figure 3.** Illustration of 12 maxillary trueness comparisons which were performed for every intraoral scanner. Every arrow symbolizes one 3D comparison. Mandibular trueness comparisons were performed in the same way for every intraoral scanner.

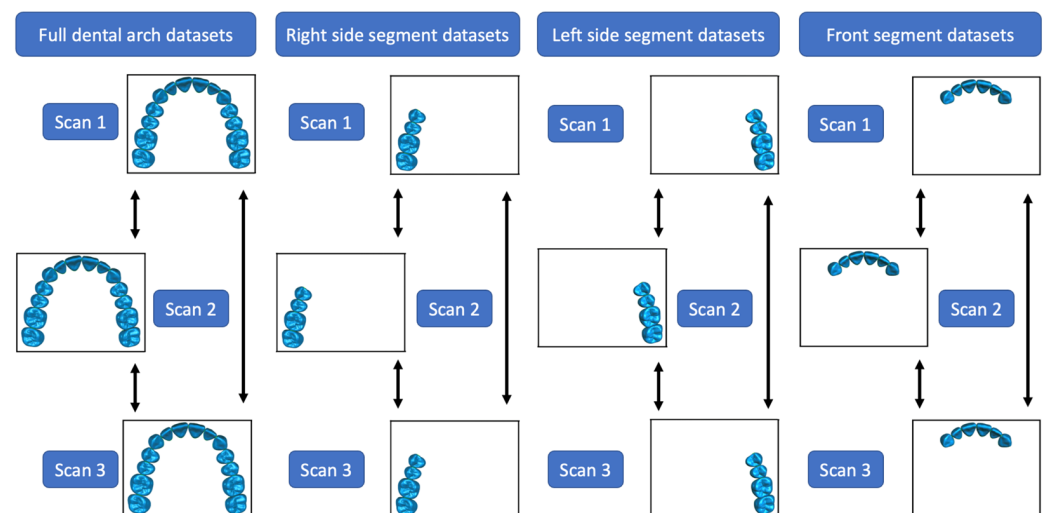


**Figure 4.** Illustration of 12 maxillary precision comparisons. The respective parts of the three scans conducted with every intraoral scanner were compared with each other. Every arrow symbolizes one 3D comparison. Mandibular precision comparisons were performed in the same way.

Subsequently, 120 trueness (24 per scanner, Figure 3) and 120 precision (24 per scanner, Figure 4) comparisons were conducted. All comparisons were carried out by 3D superimposition using the Best-Fit-Alignment algorithm in the Geomagic software.

The Best-Fit-Alignment mechanism made use of an iterative closest point algorithm, which meant that both objects first were brought into an approximately matched position before the test object was sampled. Depending on the selected sample size, a certain number of points was matched with their corresponding points on the reference scan. Both objects were brought into an approximately matched position by virtually superimposing

the reference scan and the test scan with a tolerance level of 100  $\mu\text{m}$  with a gross alignment algorithm. In a second step, both scans were superimposed as close as possible with the aid of the software's high-precision fitting algorithm, which made only fine adjustments.

The next step contained the three-dimensional comparison of the two segments. The distance of each surface point of the reference scan to its corresponding surface point of the test object was calculated. A maximum deviation of 600  $\mu\text{m}$  and a critical angle of 45° were set. For the displayed optical spectrum, 48 color segments and maximum/minimum critical values of 100/−100  $\mu\text{m}$  were set.

The results of the 3D comparisons were analyzed with statistical software (STATA 17.0, StataCorp, College Station, TX, USA). A one-way analysis of variance (ANOVA) was conducted to compute differences within groups as well as in comparison to the reference scanner. Because of various pairwise comparisons, Scheffé's method was applied for  $p$ -value adjustments. The level of statistical significance was set to  $p < 0.05$ . In addition, a visual assessment of the interproximal areas, alignment errors, tessellation and the localization of compressions and expansions of the scans was carried out with the aid of the 3D evaluation software.

### 3. Results

The five examined intraoral scanners showed statistically significant ( $p < 0.05$ ) different trueness and precision values depending on the part of the dental arch which was scanned and depending on the jaw scanned. The quality of the scanned interproximal areas as well as the number and the distribution of datapoints varied between the intraoral scanners.

#### 3.1. Full Dental Arch Scans

The full dental arch scans showed no statistically significant differences between the TR, the CS and the IT mean trueness values. However, there were statistically significant differences between the mean trueness and precision values of the full dental arch scans of the PS and all other scanners ( $p < 0.05$ , Table 2, Figure 5).

**Table 2.** Mean trueness and mean precision values  $\pm$  the standard deviations (SDs) for the full dental arch scans, maxillary and mandibular values combined.

Scanner	Trueness	Precision
	Mean Value $\pm$ SD ( $\mu\text{m}$ )	Mean Value $\pm$ SD ( $\mu\text{m}$ )
CS	29.2 $\pm$ 9.7	25.6 $\pm$ 4.8
PS	90.8 $\pm$ 31.0	95.0 $\pm$ 42.6
IT	23.5 $\pm$ 5.3	26.0 $\pm$ 7.7
TR	20.7 $\pm$ 5.8	18.8 $\pm$ 4.3
TD	58.7 $\pm$ 22.2	34.7 $\pm$ 16.5

#### 3.2. Full Dental Arch Scans: Maxilla Versus Mandibula

The CS, TR and TD showed lower mandibular complete arch mean trueness values, while the PS and IT showed lower maxillary complete arch mean trueness values. All scanners except for the TD showed lower maxillary than mandibular mean precision values in the complete dental arch segment (Table 3).

#### 3.3. Left, Right and Front Segments

The CS, TR, TD and IT showed lower mandibular mean trueness values in the left posterior, right posterior and front segment. There was no statistically significant difference between the PS mandibular and maxillary trueness values of these three segments ( $p < 0.05$ , Table 4, Figure 6). There was no statistically significant difference between mandibular and maxillary precision values for all scanners except for the IT, which showed higher mean mandibular precision values ( $p < 0.05$ , Table 4, Figure 7).

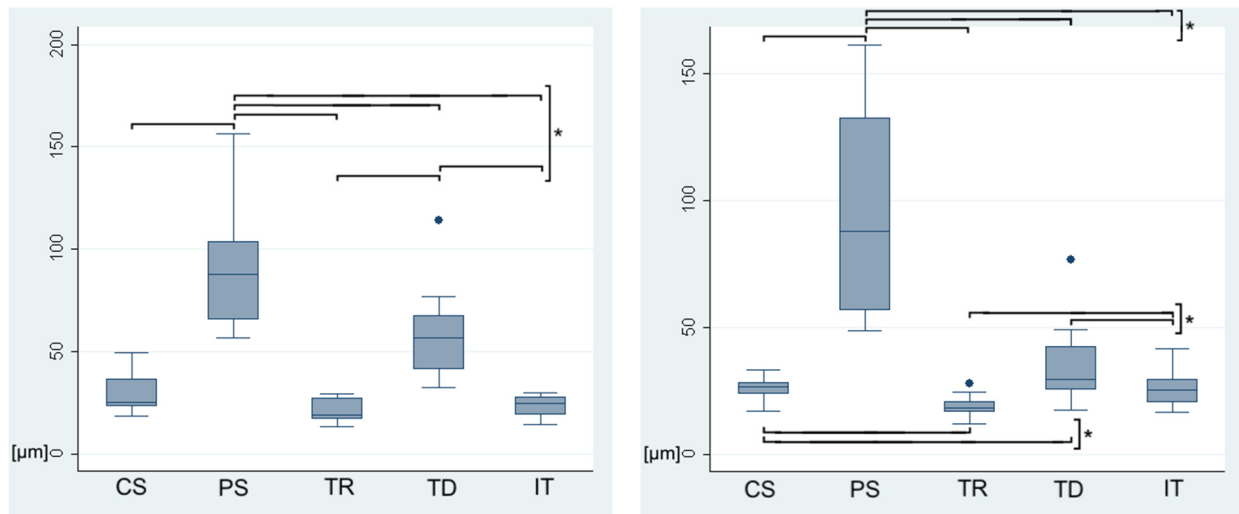


**Figure 5.** Illustration of the absolute mean trueness (**left**) and the absolute mean precision (**right**) values [ $\mu\text{m}$ ] of the full dental arch scans (maxillary and mandibular values combined, \*  $p < 0.05$ ).

**Table 3.** Mean maxillary and mean mandibular trueness and precision values  $\pm$  the standard deviations (SDs) for the full dental arch segment.

Scanner	Trueness	Precision
	Mean Value $\pm$ SD ( $\mu\text{m}$ )	Mean Value $\pm$ SD ( $\mu\text{m}$ )
CS (Maxilla)	34.0 $\pm$ 11.5	24.6 $\pm$ 6.3
CS (Mandibula)	24.4 $\pm$ 4.6	26.7 $\pm$ 3.0
PS (Maxilla)	77.5 $\pm$ 16.4	56.7 $\pm$ 7.1
PS (Mandibula)	104.1 $\pm$ 37.7	133.3 $\pm$ 20.6
IT (Maxilla)	20.9 $\pm$ 5.4	21.0 $\pm$ 3.6
IT (Mandibula)	26.1 $\pm$ 3.9	31.0 $\pm$ 7.7
TR (Maxilla)	23.8 $\pm$ 6.9	16.6 $\pm$ 3.2
TR (Mandibula)	17.7 $\pm$ 1.7	21.0 $\pm$ 4.3
TD (Maxilla)	65.4 $\pm$ 29.7	44.6 $\pm$ 18.2
TD (Mandibula)	51.9 $\pm$ 9.9	24.7 $\pm$ 5.5

**Table 4.** Mean maxillary and mandibular trueness and precision values  $\pm$  standard deviations (SDs) for the front segment, the right posterior segment and left posterior segment.

Scanner	Trueness			Precision		
	Left	Right	Front	Left	Right	Front
	Mean Value $\pm$ SD ( $\mu\text{m}$ )			Mean Value $\pm$ SD ( $\mu\text{m}$ )		
CS (Maxilla)	27.7 $\pm$ 7.9	28.8 $\pm$ 8.7	28.9 $\pm$ 8.5	20.9 $\pm$ 10.9	18.8 $\pm$ 1.3	18.3 $\pm$ 2.7
CS (Mandibula)	21.1 $\pm$ 2.7	20.5 $\pm$ 2.5	18.8 $\pm$ 3.2	22.5 $\pm$ 4.4	21.1 $\pm$ 4.1	16.0 $\pm$ 2.0
PS (Maxilla)	44.5 $\pm$ 16.5	46.0 $\pm$ 9.3	63.4 $\pm$ 32.1	38.1 $\pm$ 11.0	30.0 $\pm$ 3.1	56.4 $\pm$ 13.4
PS (Mandibula)	53.2 $\pm$ 33.7	44.6 $\pm$ 17.7	59.5 $\pm$ 33.1	40.4 $\pm$ 5.6	46.5 $\pm$ 20.4	52.8 $\pm$ 9.8
IT (Maxilla)	17.5 $\pm$ 5.2	18.9 $\pm$ 6.4	20.8 $\pm$ 4.2	16.4 $\pm$ 4.9	17.8 $\pm$ 4.2	19.3 $\pm$ 6.3
IT (Mandibula)	11.2 $\pm$ 2.3	13.4 $\pm$ 1.5	19.7 $\pm$ 6.8	24.2 $\pm$ 9.8	18.1 $\pm$ 5.0	31.1 $\pm$ 8.5
TR (Maxilla)	20.8 $\pm$ 5.1	21.5 $\pm$ 7.8	21.7 $\pm$ 5.9	15.1 $\pm$ 4.2	10.0 $\pm$ 2.0	15.3 $\pm$ 2.5
TR (Mandibula)	12.8 $\pm$ 4.4	14.3 $\pm$ 1.6	15.9 $\pm$ 0.9	15.5 $\pm$ 4.1	12.8 $\pm$ 3.1	13.2 $\pm$ 2.9
TD (Maxilla)	31.2 $\pm$ 13.4	35.3 $\pm$ 16.7	34.1 $\pm$ 10.9	11.7 $\pm$ 2.4	11.7 $\pm$ 1.9	17.8 $\pm$ 4.9
TD (Mandibula)	24.0 $\pm$ 3.1	28.0 $\pm$ 4.9	25.0 $\pm$ 2.0	10.6 $\pm$ 2.4	14.7 $\pm$ 2.8	11.9 $\pm$ 1.7

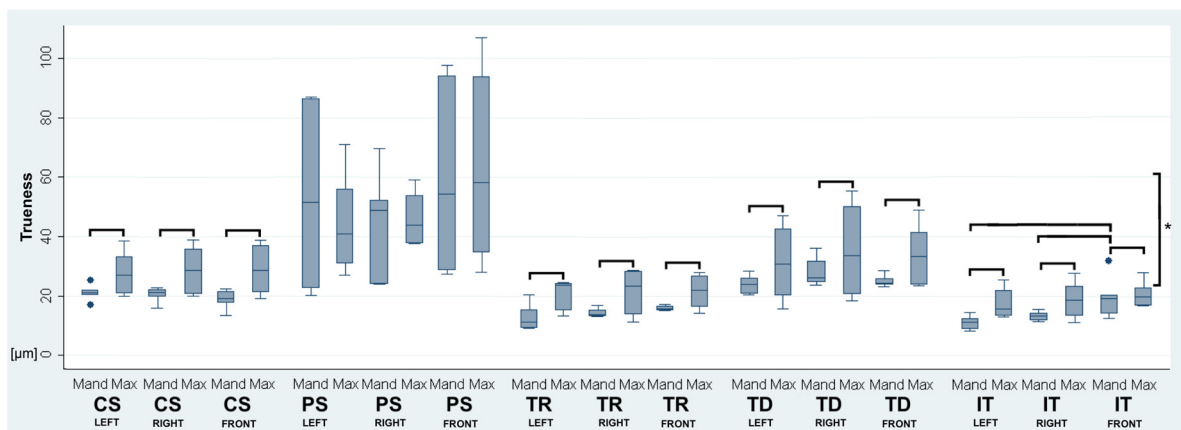


**Figure 6.** Illustration of the mandibular and maxillary trueness values of the front segment, the right posterior segment and left posterior segment (\*  $p < 0.05$ ).

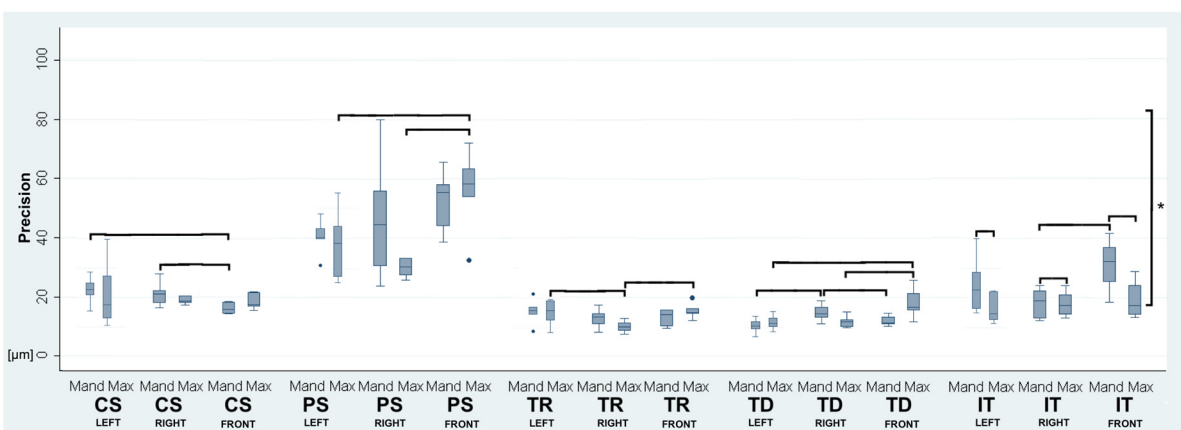


**Figure 7.** Illustration of the mandibular and maxillary precision values of the front segment, the right posterior and left posterior segment (\*  $p < 0.05$ ).

### 3.4. 3D Deviations

All CS maxillary scans showed compressed areas in the labial front and the buccal side parts. In addition, all maxillary scans showed compressed areas in the oral region from tooth 11 to 26 and 14 to 17. For the CS scanner, areas of compression and areas of expansion were more evenly distributed in mandibular scans compared to maxillary scans, which showed more areas of compression.

All maxillary PS scans showed areas of compression in the vestibular parts of the teeth 16, 17 and 27. All mandibular scans showed areas of expansion in the left vestibular front region (32 and 33) and the oral front region (42 to 33, Figure 8). Overall, areas of expansion were more dominant than areas of compression in PS scan files.

IT maxillary scans showed areas of compression on all vestibular surfaces as well as on the distal parts of teeth 17 and 27 and areas of compression on the occlusal parts of 15, 16 and 25, 26. In the IT mandibular scans, areas of expansion in the vestibular parts of teeth 47, 46, 34 and 35, as well as on the distal part of 47, were observed. All three mandibular scans showed an occlusal compression on tooth 46. In the maxillary IT scans, areas of compression were more dominant than areas of expansion. Areas of compression and areas of expansion were more evenly distributed in mandibular scans.

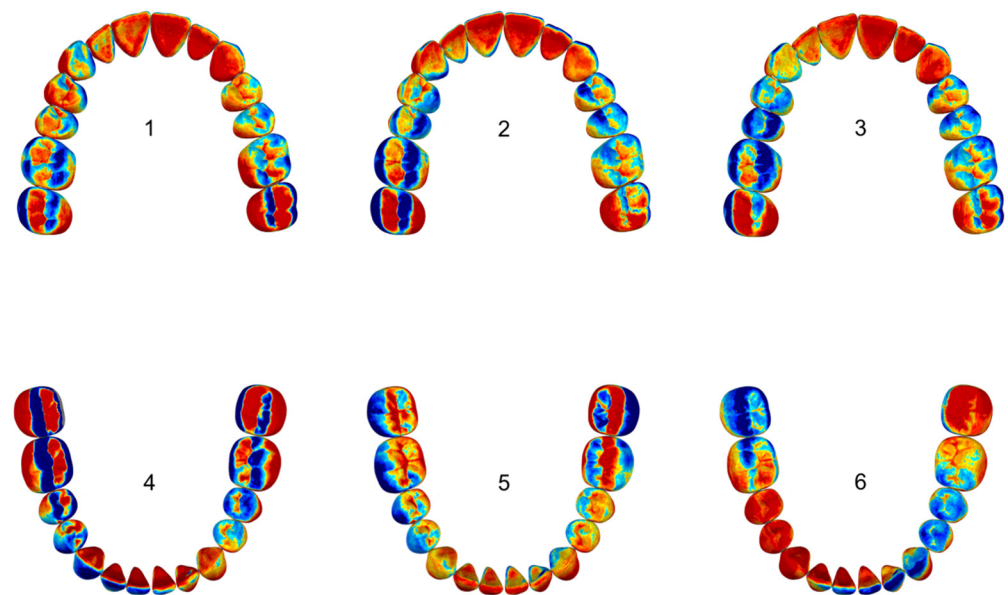


**Figure 8.** Illustration of the PS maxillary and mandibular trueness deviation pattern (warmer colors indicating areas of expansion and cooler colors indicating areas of compression).

On all TR vestibular and oral maxillary surfaces, as well as on the incisal surface of tooth 11, areas of compression were predominant. In the mandibular scans, areas of compression were dominant in the oral parts of the premolar regions of both sides of the dental arch as well as in the right front region (43, 42). Areas of compression were more dominant in maxillary scans compared to mandibular scan files, where areas of compression and areas of expansion were more evenly distributed (Figure 9).

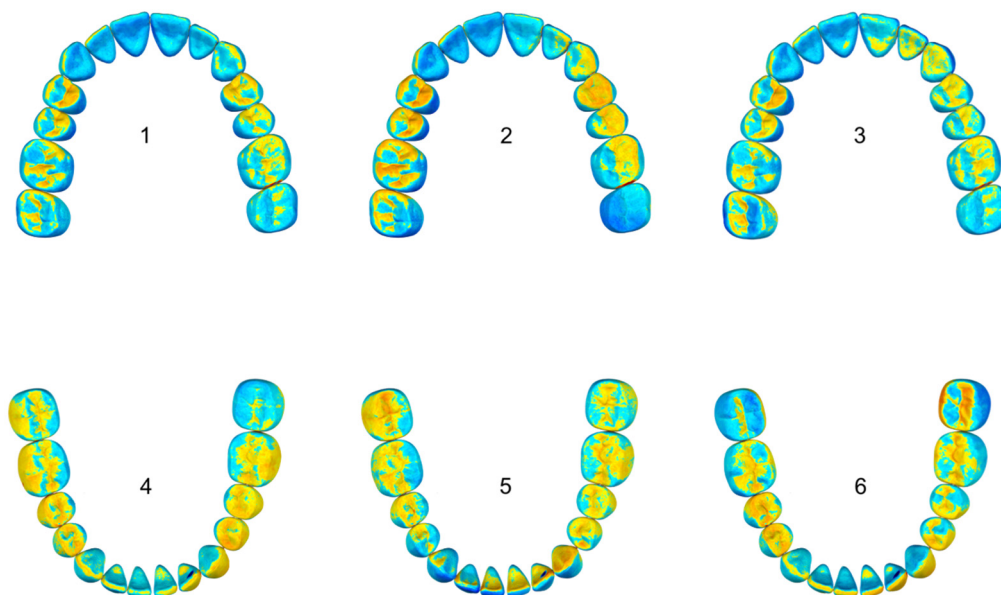


**Figure 9.** Illustration of the TR maxillary and mandibular trueness deviation pattern (warmer colors indicating areas of expansion and cooler colors indicating areas of compression).

Maxillary scans of the TD showed areas of predominant compression on all vestibular surfaces as well as distal of 17 and 27. All mandibular scans showed areas of compression on the vestibular surfaces as well as on the distal surfaces of 47 and 37. Mandibular scans seemed to be compressed towards the center of the dental arch (Figure 10). Both jaws showed common areas of compression on all vestibular surfaces as well as on the distal

parts of the last molars. In addition, both jaws showed areas of oral expansion in the front region from 12/42 to 23/33.

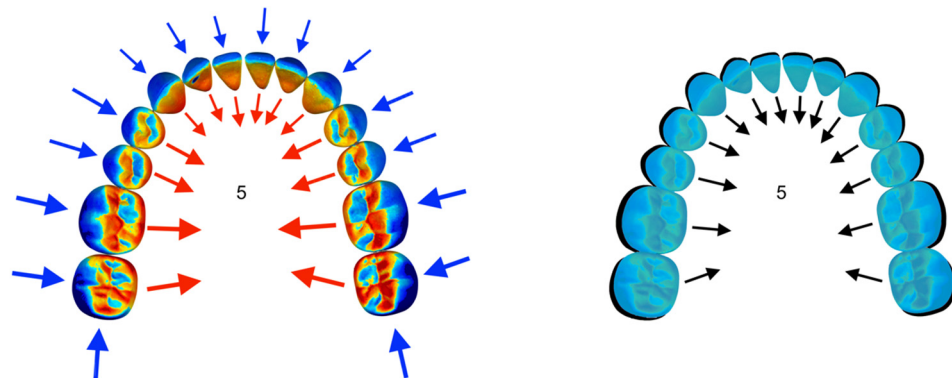


**Figure 10.** Illustration of the horizontal deviations of scan 5 of the TD. **(Left side):** Red arrows indicate areas of expansion and blue arrows indicate areas of compression. **(Right side):** Schematic representation of the dental arch distortion.

### 3.5. Interproximal Areas

Scan results of interproximal areas were worse than the results of the other parts of the full arch scans. A total of 31% of interproximal areas were blocked in TR maxillary scans, which was 21% more than in mandibular scans (Figure 11).

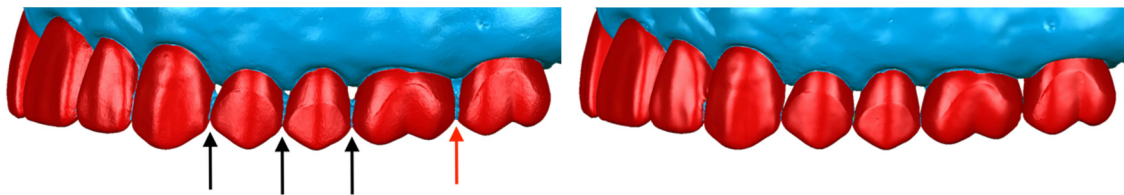


**Figure 11.** **(Left):** Most TR maxillary interproximal areas were captured smaller (black arrows) or completely blocked (red arrow). **(Right):** Reference scan with free interproximal areas.

In total, 64% of interproximal areas were blocked in CS maxillary scans, which was 28% more than in mandibular scans, and 100% of interproximal areas were blocked in IT maxillary scans, which was 13% more than in mandibular scans. Parts of all interproximal tooth surfaces were missing in TD scans (Figure 12).

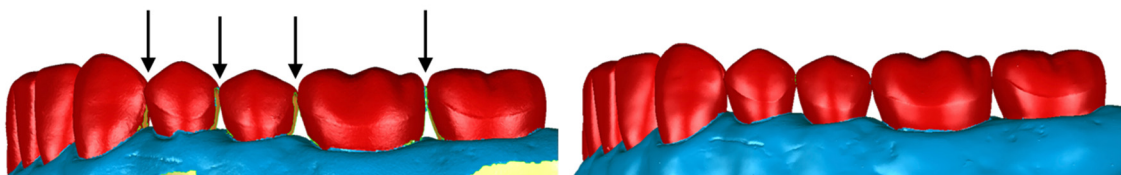


**Figure 12.** **(Left):** Black arrows indicate missing interproximal areas of TD scans. **(Right):** Reference scan with entirely captured interproximal areas.

### 3.6. Number and Distribution of Datapoints and Outliers

The scanner with the highest number of datapoints was the PS, while the CS showed the lowest number of datapoints (Table 5).

**Table 5.** Illustration of the scanners' different maxillary and mandibular average number of datapoints which belonged to tooth surfaces. Average values were rounded to whole numbers. In brackets: highest and lowest value of the respective intraoral scanner's scan files.

Scanner	Full Arch	Front Segment	Right Side Segment	Left Side Segment
	Number of Datapoints			
Reference (Maxilla)	400,149	137,490	123,344	139,376
Reference (Mandibula)	306,242	92,101	115,615	98,593
CS (Maxilla)	70,046 (70,586–69,691)	26,551 (27,010–26,303)	22,042 (22,581–21,546)	21,423 (21,934–20,983)
CS (Mandibula)	65,005 (66,099–64,115)	21,186 (21,550–20,540)	21,388 (21,856–20,903)	22,434 (22,858–21,747)
PS (Maxilla)	162,649 (163,987–161,689)	58,909 (60,733–57,828)	52,249 (52,746–51,709)	51,489 (51,562–51,354)
PS (Mandibula)	148,577 (149,020–148,270)	44,777 (45,134–44,563)	51,191 (51,729–50,670)	52,620 (53,204–51,577)
IT (Maxilla)	82,147 (88,124–77,413)	28,455 (30,871–26,224)	26,259 (29,167–24,368)	27,390 (28,088–26,736)
IT (Mandibula)	72,575 (77,276–70,029)	21,213 (23,598–19,088)	25,617 (26,880–24,495)	25,675 (26,800–24,968)
TR (Maxilla)	169,294 (169,730–168,868)	57,687 (57,888–57,579)	56,036 (56,383–55,527)	55,428 (55,787–54,790)
TR (Mandibula)	144,721 (149,068–141,864)	41,933 (43,095–41,236)	50,684 (52,339–49,542)	52,079 (53,601–51,050)
TD (Maxilla)	141,761 (142,367–140,987)	52,054 (52,364–51,497)	45,031 (45,307–44,692)	44,678 (44,876–44,396)
TD (Mandibula)	128,186 (128,824–127,300)	40,140 (40,361–39,952)	43,702 (44,342–42,917)	44,346 (44,615–44,149)

The intraoral scanners generated different numbers of outliers (Table 6). CS and TD scans showed uniform tessellation (Figure 13) while IT, TR and PS scans showed non-uniform tessellation (Figure 14).

**Table 6.** Average reported number of maxillary and mandibular outliers in the whole dental arch segment trueness comparisons.

Scanner	Number of Outliers
CS (Maxilla)	157
CS (Mandibula)	101
PS (Maxilla)	413
PS (Mandibula)	919
IT (Maxilla)	259
IT (Mandibula)	210
TR (Maxilla)	376
TR (Mandibula)	265
TD (Maxilla)	50
TD (Mandibula)	62

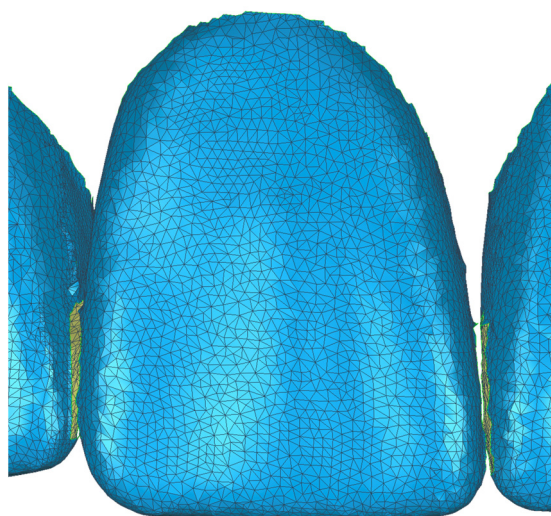


**Figure 13.** Illustration of the CS virtual triangles of tooth 11 of scan 1. The dimensions of a virtual triangle are defined by the location of three datapoints, which were generated during the scanning process. The surface of a 3D scan is composed of multiple virtual triangles.

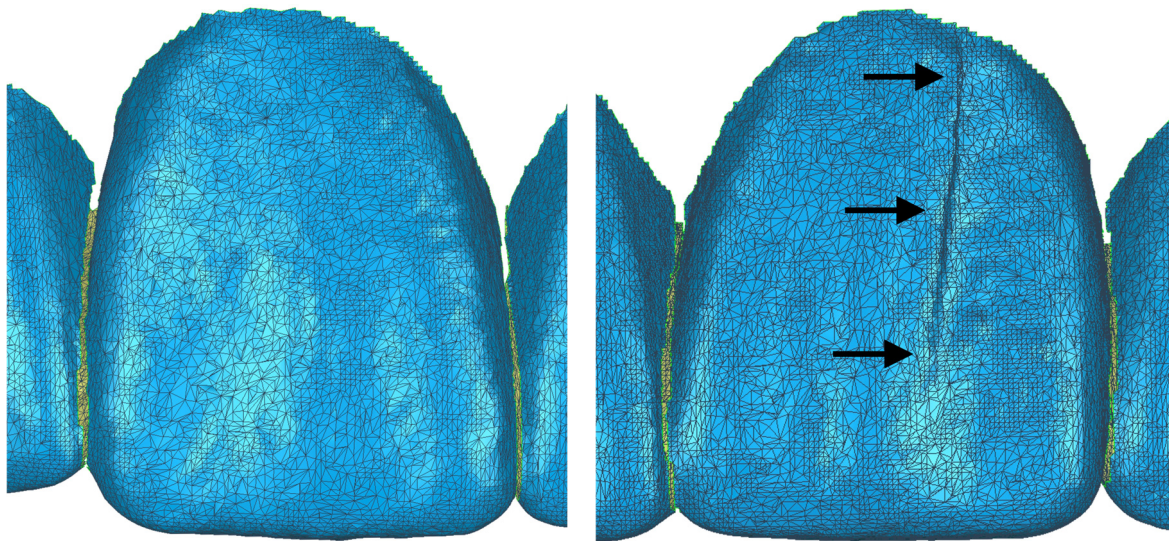


**Figure 14.** Illustration of the PS virtual triangles of tooth 11 from scan number 1 and of tooth 21 from scan number 3. Black arrows indicate an alignment error.

#### 4. Discussion

The *in vitro* approach of this study made it possible to provide similar, controllable scanning conditions for all scanners. *In vivo* scans are more difficult to perform because of limited space in the oral cavity, patient movements, moisture and soft tissue obstacles. In addition, the oral cavity is too small for the reference scanner used in this study. As reported in another study, extraoral long span scans with intraoral scanners can be more accurate than intraoral long span scans [25]. This has to be considered when interpreting the results of this study. In order not to influence the intraoral scanners' accuracy in a negative way, a non-translucent plastic material with natural tooth-colored teeth was chosen for the reference models in this study. More translucent materials such as enamel, which are present during patient care, seem to have a negative effect on the accuracy of many intraoral scanners [26]. For these reasons, the tested intraoral scanners are expected to provide lower accuracy under clinical conditions.

The reference scanner has been reported to be true to 3  $\mu\text{m}$  [26–28], which is important because all intraoral scans have been compared to the reference scans during the trueness evaluations. The scans in this study were performed by a single, experienced dentist in order to not influence the scanning process in a negative way. The method of best-fit 3D superimposition was chosen as the most suitable because this study examined the ability of intraoral scanners to scan natural tooth shapes [29,30].

The limit of clinical acceptance for trueness values was set to 50  $\mu\text{m}$ . This limit was chosen because intraoral appliances with higher differences to a patient's tooth positions can impair blood flow in the periodontal ligament [31,32]. This can be seen as the upper limit of clinical acceptance assuming the theoretical fact that no further inaccuracies are added on top of the intraoral scan's inaccuracy along the clinical workflow.

A major reason for the lower trueness of the CS compared to the TR seemed to be the lower number of datapoints, which can lead to higher calculated deviations of the reference scan file after 3D superimposition and thus to higher trueness values. However, there was no statistically significant difference between the full arch mean trueness of the CS, IT and TR ( $p < 0.05$ , Table 2, Figure 5). By analogy with this study, another *in vitro* study which evaluated the successors of the CS and TR by scanning a full dentate maxilla with unprepared teeth found comparable mean trueness values of  $26.9 \pm 15.9 \mu\text{m}$  with the CS 3600,  $27.7 \pm 6.8 \mu\text{m}$  with the TRIOS 3 and  $20.8 \pm 6.2 \mu\text{m}$  with the TRIOS 4 [33]. In line with this, an *in vivo* study evaluating the CS 3600 and the TRIOS 3 in scanning the maxillary arch found comparable trueness levels between the two successor models [34]. Another *in vitro* study, however, which evaluated the effect of artificial saliva on COIM of full arch

scans with unprepared teeth, found higher trueness values for the CS 3600 and TRIOS 3 than the present investigation [35]. These findings indicate that proper moisture control is more important than further developed scanner generations.

The PS scanner works with the principle of optical triangulation and thus faced similar technical challenges to the CS. However, the CS can be stabilized on neighboring structures before a single scan image is taken, which has probably contributed to lower trueness and precision values of the CS compared to the PS. The PS constantly has to be moved above the scanned object at a certain focal distance because it automatically takes scan images at a higher rate compared to the CS [36].

Another examination reported the highest PS distortions in the apicocoronal axis [37]. In the present study, PS deviations were more evenly distributed over the surface of the teeth. In accordance with the present investigation, other authors also reported surface irregularities and a high number of datapoints for the PS [30]. The PS showed the highest numbers of outliers in this study (Table 6). This contributed to higher trueness and precision values of the PS in comparison to the other intraoral scanners tested in this study. The main reason for the lower trueness and precision of the PS compared to the other scanners seemed to be alignment mistakes because the PS showed significantly higher accuracy in the front, left posterior and right posterior segment than in the whole dental arch scans. In a recent study, median 3D full arch trueness values of the latest Planmeca scanner generation were higher than the respective values of the latest generation of TRIOS scanners [21]. Thus, in accordance with the present study, it can be stated that TRIOS scanners benefited more from generation changes than Planmeca scanners. The PS always showed the lowest accuracy in the front segment, presumably because the front has less geometrical information than the side sectors of the dental arch. This probably contributed to alignment mistakes (Figure 14). The reason for the better acquisition of maxillary interproximal areas has yet to be identified. More difficult handling, non-uniform tessellation and the highest number of reported outliers in this study have contributed to the lower accuracy of the PS compared to the CS despite the fact that both scanners used the same basic measurement principle of optical triangulation. The PS did not reach a trueness level of clinical acceptance in full arch scans in this study.

Similar to the point-and-click image acquisition mode of the CS, the IT used single images for the data acquisition. In triangulation-based scanners, light reflections from three different angles are measured. Depending on the reflective characteristics of the surface, the reflecting angle and thus the measured distance can be different. In contrast, the IT used the measurement principle of parallel confocal microscopy and only measured light rays that were reflected to its respective focal plane and focused on the optical sensor [38]. However, the presence of a color wheel can lead to mechanical irritations during the scanning process due to vibrations and to a limited speed of data acquisition due to a limited switching speed of the color wheel [5]. Furthermore, confocal sensors are sensitive to temperature changes and are only calibrated for a certain temperature. In addition, only certain wavelengths can be measured, which limits the number of possible measurement distances [39]. Despite these technical challenges, the IT performed among the top three scanners concerning mean accuracy of the full dental arch. In contrast to the PS and TD, the IT showed comparably small differences between full arch and partial arch precision. A certain deviation pattern for iTero with larger deviations at one distal end of the dental arch was reported by other authors [40]. This trueness deviation pattern could not be confirmed in the study at hand as most higher trueness deviations were located on both ends of the dental arch and in the front area. Another examination reported a resolution of 34.2 datapoints per mm<sup>2</sup> for the iTero, which is very similar to the average resolution determined in this study of 31.3 datapoints per mm<sup>2</sup>. By analogy with the present study, no relationship between trueness and resolution was found for the IT [28]. Despite a higher number of outliers and non-uniform tessellation compared to the CS, the IT showed the lowest maxillary full arch mean trueness values of all intraoral scanners tested in this study. In contrast, the IT showed 44% more blocked interproximal areas than the other tested point-and-click system

(CS). Possibly this was due to hardware differences as the CS used active triangulation technology.

In a recent study, the mean mandibular and maxillary trueness values ranged from 32 to 48  $\mu\text{m}$  with the iTero Element 5D, which is the latest iTero model generation [41]. The higher mean trueness values of the latest iTero model generation compared to the values of the iTero scanner used in this study were probably caused by the circumstance that natural teeth with filling materials were more difficult to scan. Nonetheless, this highlights that newer model generations do not necessarily produce scans with a higher trueness.

An important feature of the TR is that, while scanning, the focal plane is changed in a periodic pattern without changing the scanner's head distance from the scanned object [38]. A high contrast is achieved as every point of the scanned surface is only scanned when the point is in focus and when it shows a maximum level of correlation in the scanner's optical field on the digital sensor. Scanning errors might occur when changing of the focal plane overlaps with changing positions of the operator's arm. This error is supposed to be minimized by a high speed of focal plane changes and very short data acquisition time [42]. The TR showed the highest number of datapoints in maxillary scans in the study at hand and the second highest number of datapoints in mandibular scans. However, the TR also exhibited the second highest number of outliers. Despite a higher number of outliers compared to the IT, CS and TD and non-uniform tessellation, The TR showed the highest overall trueness and precision of all intraoral scanners tested in this study. Nonetheless, there was no statistically significant difference between the overall mean trueness and precision of the TR, IT and CS ( $p < 0.05$ ). The TR showed significantly less blocked interproximal areas than the other scanner, which used parallel confocal microscopy in this study (IT). A major reason for this might be that the TR is a video-based system, while the IT works with single pictures. Mean trueness values of the TRIOS 3 and 4 in another in vitro study, which also made use of a full arch reference model with unprepared teeth, were higher than with the TRIOS scanner tested in this study [33]. The TRIOS 4 also produced higher mean trueness values in a recent study [41]. Thus, contrary to a study by Schmalzl et al. [21], which used a full arch model with missing and prepared teeth, TRIOS scanners did not show a significant trueness improvement in newer model generations.

Despite the need for reflective coating and the risk of uneven powder application, the TD has previously been shown to work very accurately [36,43,44]. The TD delivers 3D images in a real-time video sequence by using a blue-LED-light wavefront sampling technique. The image acquisition process required a uniform surface, which was provided by reflective coating with titanium oxide powder. Identical reflecting properties were necessary because light reflections from different angles, like in triangulation-based optical sensors, are focused on optical sensors [36,45]. The scanner used a rotating device, which is located in the front of the sensor. This device allows images of the same location from different angles and thus works like different cameras taking 2D images of the same object which are computed together to a single 3D picture [46]. Moving mechanical parts like the built-in rotating aperture and incorrectly applied reflective coating were potential sources of error for the scanning process. On the other hand, reflective coating can also increase scanning accuracy because it creates a more uniform reflecting surface than tooth surfaces composed of different materials [29]. The missing interproximal parts of TD scans might be due to insufficient powder application. The reference scanner, however, also needed reflective coating and accurately scanned interproximal areas. Thus, insufficient powder application most likely was not the reason for the insufficient acquisition of interproximal areas with the TD. The better acquisition of interproximal areas with the reference scanner might be linked to the different scanning principles of the two scanners. In conclusion, in vitro, apart from interproximal areas, the TD exhibited clinically acceptable trueness only in the front, the left posterior and the right posterior segment. Full arch trueness did not meet the required level of clinical acceptance of 50  $\mu\text{m}$ . The main reason for the TD's

higher whole arch trueness values compared to the individual sector values seemed to be alignment errors.

In general, a higher amount of geometrical information has been reported to lead to intraoral scans with higher accuracy [47]. On the other hand, digital impressions with large spans are associated with a higher number of stitching errors [48]. Mandibular trueness in this study in comparison to maxillary trueness was higher for all intraoral scanners except for the PS, which did not show statistically significant differences between maxillary and mandibular trueness ( $p < 0.05$ , Table 4, Figure 6). Only the mandibular precision of the IT was lower compared to the scanner's maxillary precision ( $p < 0.05$ , Table 4, Figure 7). The maxillary dental arch is longer than the mandibular arch, and it provides a higher amount of geometrical information because of larger maxillary front teeth. Thus, the number of alignment mistakes due to the longer maxillary dental arch must have outweighed the benefits of a higher amount of maxillary geometrical information in the front region.

The leading cause for the lower full arch trueness of the PS and TD compared to the other intraoral scanners tested in this study seemed to be alignment errors because their individual segment trueness values were significantly lower than their full arch trueness values (Table 2, Table 4).

It was not possible to fully explain the different results of the intraoral scanners used in this study because detailed information about the scanners' hardware and software is not publicly available.

## 5. Conclusions

COIM is important as the first step in a digital workflow for the production of orthodontic appliances. However, apart from interproximal areas, clinically acceptable maxillary and mandibular full arch trueness was only achieved by the CS 3500, the iTero HD2.9 and the TRIOS Standard intraoral scanner. The acquisition of interproximal areas showed the need for improvement across all scanning systems. The leading cause for the lower trueness of full arch scans compared to partial arch scans seemed to be alignment errors. In the field of COIM, further research on the accuracy under clinical conditions and on the acquisition of interproximal areas is needed.

**Author Contributions:** Conceptualization, L.D. and S.B.M.P.; methodology, L.D. and S.B.M.P.; software, L.D., S.B.M.P. and K.V.; validation, L.D., S.B.M.P., K.V. and R.J.K.; formal analysis, L.D. and K.V.; investigation, L.D. and S.B.M.P.; resources, L.D., S.B.M.P. and K.V.; data curation, L.D., S.B.M.P. and K.V.; writing—original draft preparation, L.D.; writing—review and editing, L.D., S.B.M.P., K.V. and R.J.K.; visualization, L.D.; supervision, S.B.M.P. and R.J.K.; project administration, L.D. and S.B.M.P.; funding acquisition, L.D. All authors have read and agreed to the published version of the manuscript.

**Funding:** The publication was supported by the Open Access Publication Fund of the University of Freiburg.

**Institutional Review Board Statement:** Not applicable.

**Informed Consent Statement:** Not applicable.

**Data Availability Statement:** The data underlying this article will be shared on reasonable request to the corresponding author.

**Conflicts of Interest:** The authors declare no conflicts of interests.

## References

1. Ender, A.; Mehl, A. Influence of scanning strategies on the accuracy of digital intraoral scanning systems. *Int. J. Comput. Dent.* **2013**, *16*, 11–21.
2. Kachalia, P.R.; Geissberger, M.J. Dentistry a la carte: In-office CAD/CAM technology. *J. Calif. Dent. Assoc.* **2010**, *38*, 323–330. [[CrossRef](#)]
3. Stanley, M.; Paz, A.G.; Miguel, I.; Coachman, C. Fully digital workflow, integrating dental scan, smile design and CAD-CAM: Case report. *BMC Oral Health* **2018**, *18*, 134. [[CrossRef](#)]

4. Aswani, K.; Wankhade, S.; Khalikar, A.; Deogade, S. Accuracy of an intraoral digital impression: A review. *J. Indian Prosthodont. Soc.* **2020**, *20*, 27–37. [[CrossRef](#)]
5. Patzelt, S.B.; Emmanouilidi, A.; Stampf, S.; Strub, J.R.; Att, W. Accuracy of full-arch scans using intraoral scanners. *Clin. Oral Investig.* **2014**, *18*, 1687–1694. [[CrossRef](#)]
6. Patzelt, S.B.; Lamprinos, C.; Stampf, S.; Att, W. The time efficiency of intraoral scanners: An in vitro comparative study. *J. Am. Dent. Assoc.* **2014**, *145*, 542–551. [[CrossRef](#)] [[PubMed](#)]
7. Yuzbasioglu, E.; Kurt, H.; Turunc, R.; Bilir, H. Comparison of digital and conventional impression techniques: Evaluation of patients' perception, treatment comfort, effectiveness and clinical outcomes. *BMC Oral Health* **2014**, *14*, 10. [[CrossRef](#)]
8. Saccomanno, S.; Saran, S.; Vanella, V.; Mastrapasqua, R.F.; Raffaelli, L.; Levrini, L. The potential of digital impression in orthodontics. *Dent. J.* **2022**, *10*, 147. [[CrossRef](#)] [[PubMed](#)]
9. Retrouvey, J.-M.; Kader, E.; Caron, E.; Tamimi, F.; Light, N. *Printing Orthodontic Retainers Using CAD/CAM Technology*; McGill University: Montreal, QC, Canada, 2013.
10. Wiechmann, D.; Rummel, V.; Thalheim, A.; Simon, J.S.; Wiechmann, L. Customized brackets and archwires for lingual orthodontic treatment. *Am. J. Orthod. Dentofac. Orthop.* **2003**, *124*, 593–599. [[CrossRef](#)] [[PubMed](#)]
11. Zimmermann, M. Die digitale Abformung mit dem Intraoralscanner: Intraorale Scansysteme: Kaufentscheidungen und System Übersicht. *ZMK* **2016**, *32*, 166–172. [[CrossRef](#)]
12. Gimenez, C.M.M. Digital technologies and CAD/CAM systems applied to lingual orthodontics: The future is already a reality. *Dent. Press J. Orthod.* **2011**, *16*, 6. [[CrossRef](#)]
13. Brown, M.W.; Koroluk, L.; Ko, C.C.; Zhang, K.; Chen, M.; Nguyen, T. Effectiveness and efficiency of a CAD/CAM orthodontic bracket system. *Am. J. Orthod. Dentofac. Orthop.* **2015**, *148*, 1067–1074. [[CrossRef](#)] [[PubMed](#)]
14. Wiechmann, D. A new bracket system for lingual orthodontic treatment. Part 2: First clinical experiences and further development. *J. Orofac. Orthop.* **2003**, *64*, 372–388. [[CrossRef](#)] [[PubMed](#)]
15. Wolf, M.; Schumacher, P.; Jäger, F.; Wego, J.; Fritz, U.; Korbmacher-Steiner, H.; Jäger, A.; Schauseil, M. Novel lingual retainer created using CAD/CAM technology: Evaluation of its positioning accuracy. *J. Orofac. Orthop.* **2015**, *76*, 164–174. [[CrossRef](#)]
16. Wilmes, B.; Willmann, J.H.; Drescher, D. Full Digital Workflow. *Kieferorthopädie Nachrichten* **2021**, *13*, 6–10.
17. Layman, B. Digital Bracket Placement for Indirect Bonding. *J. Clin. Orthod.* **2019**, *53*, 387–396.
18. Christopoulou, I.; Kaklamanos, E.G.; Makrygiannakis, M.A.; Bitsanis, I.; Perlea, P.; Tsolakis, A.I. Intraoral Scanners in Orthodontics: A Critical Review. *Int. J. Environ. Res. Public Health* **2022**, *19*, 1407. [[CrossRef](#)]
19. Yoon, J.H.; Yu, H.S.; Choi, Y.; Choi, T.H.; Choi, S.H.; Cha, J.Y. Model Analysis of Digital Models in Moderate to Severe Crowding: In Vivo Validation and Clinical Application. *BioMed Res. Int.* **2018**, *2018*, 8414605. [[CrossRef](#)]
20. Michou, S.; Lambach, M.S.; Ntovas, P.; Benetti, A.R.; Bakhshandeh, A.; Rahiotis, C.; Ekstrand, K.R. Automated caries detection in vivo using a 3D intraoral scanner. *Sci. Rep.* **2021**, *11*, 21276. [[CrossRef](#)] [[PubMed](#)]
21. Schmalzl, J.; Róth, I.; Borbély, J.; Hermann, P.; Vecsei, B. The effect of generation change on the accuracy of full arch digital impressions. *BMC Oral Health* **2023**, *23*, 766. [[CrossRef](#)] [[PubMed](#)]
22. Schmalzl, J.; Róth, I.; Borbély, J.; Hermann, P.; Vecsei, B. The impact of software updates on accuracy of intraoral scanners. *BMC Oral Health* **2023**, *23*, 219. [[CrossRef](#)]
23. Alkadi, L. A Comprehensive Review of Factors That Influence the Accuracy of Intraoral Scanners. *Diagnostics* **2023**, *13*, 3291. [[CrossRef](#)] [[PubMed](#)]
24. ISO 5725-1:1994(en); International Organization for Standardization. Accuracy (Trueness and Precision) of Measurement Methods and Results—Part 1: General Principles and Definitions. International Organization for Standardization: Geneva, Switzerland, 1994.
25. Kernen, F.; Schlager, S.; Seidel Alvarez, V.; Mehrhof, J.; Vach, K.; Kohal, R.; Nelson, K.; Flügge, T. Accuracy of intraoral scans: An in vivo study of different scanning devices. *J. Prosthet. Dent.* **2022**, *128*, 1303–1309. [[CrossRef](#)] [[PubMed](#)]
26. Dutton, E.; Ludlow, M.; Mennito, A.; Kelly, A.; Evans, Z.; Culp, A.; Kessler, R.; Renne, W. The effect different substrates have on the trueness and precision of eight different intraoral scanners. *J. Esthet. Restor. Dent.* **2020**, *32*, 204–218. [[CrossRef](#)] [[PubMed](#)]
27. Baghani, M.T.; Shayegh, S.S.; Johnston, W.M.; Shidfar, S.; Hakimaneh, S.M.R. In vitro evaluation of the accuracy and precision of intraoral and extraoral complete-arch scans. *J. Prosthet. Dent.* **2021**, *126*, 665–670. [[CrossRef](#)]
28. Medina-Sotomayor, P.; Pascual-Moscardó, A.; Camps, I. Relationship between resolution and accuracy of four intraoral scanners in complete-arch impressions. *J. Clin. Exp. Dent.* **2018**, *10*, 361–366. [[CrossRef](#)]
29. Ender, A.; Zimmermann, M.; Attin, T.; Mehl, A. In vivo precision of conventional and digital methods for obtaining quadrant dental impressions. *Clin. Oral Investig.* **2016**, *20*, 1495–1504. [[CrossRef](#)]
30. Kim, R.J.; Park, J.M.; Shim, J.S. Accuracy of 9 intraoral scanners for complete-arch image acquisition: A qualitative and quantitative evaluation. *J. Prosthet. Dent.* **2018**, *120*, 895–903. [[CrossRef](#)] [[PubMed](#)]
31. Cuoghi, O.A.; Tondelli, P.M.; Aiello, C.A.; Mendonça, M.R.; Costa, S.C. Importance of periodontal ligament thickness. *Braz. Oral Res.* **2013**, *27*, 76–79. [[CrossRef](#)]
32. Mortazavi, H.; Baharvand, M. Review of common conditions associated with periodontal ligament widening. *Imaging Sci. Dent.* **2016**, *46*, 229–237. [[CrossRef](#)]
33. Nulty, A.B. A comparison of full arch trueness and precision of nine intra-oral digital scanners and four lab digital scanners. *Dent. J.* **2021**, *9*, 75. [[CrossRef](#)] [[PubMed](#)]

34. Winkler, J.; Gkantidis, N. Trueness and precision of intraoral scanners in the maxillary dental arch: An in vivo analysis. *Sci. Rep.* **2020**, *10*, 1172. [[CrossRef](#)]
35. Song, J.; Kim, M. Accuracy on scanned images of full arch models with orthodontic brackets by various intraoral scanners in the presence of artificial saliva. *BioMed Res. Int.* **2020**, *2020*, 2920804. [[CrossRef](#)] [[PubMed](#)]
36. Hack, G.D.; Patzelt, S.B.M. Evaluation of the Accuracy of Six Intraoral Scanning Devices: An in-vitro Investigation. *ADA Prof. Prod. Rev.* **2015**, *10*, 1–5.
37. Vag, J.; Nagy, Z.; Simon, B.; Mikolicz, A.; Kövér, E.; Mennito, A.; Evans, Z.; Renne, W. A novel method for complex three-dimensional evaluation of intraoral scanner accuracy. *Int. J. Comput. Dent.* **2019**, *22*, 239–249. [[PubMed](#)]
38. Logozzo, S.; Franceschini, G.; Kilpelä, A.; Caponi, M.; Governi, L.; Blois, L. A Comparative Analysis of Intraoral 3D Digital Scanners for Restorative Dentistry. *Internet J. Med. Technol.* **2008**, *5*, 1–18.
39. Berkovic, G.; Shafir, E. Optical methods for distance and displacement measurements. *Adv. Opt. Photonics* **2012**, *4*, 441–471. [[CrossRef](#)]
40. Ender, A.; Mehl, A. In-vitro evaluation of the accuracy of conventional and digital methods of obtaining full-arch dental impressions. *Quintessence Int.* **2015**, *46*, 9–17. [[CrossRef](#)]
41. Vag, J.; Stevens, C.D.; Badahman, M.H.; Ludlow, M.; Sharp, M.; Brenes, C.; Mennito, A.; Renne, W. Trueness and precision of complete arch dentate digital models produced by intraoral and desktop scanners: An ex-vivo study. *J. Dent.* **2023**, *139*, 104764. [[CrossRef](#)]
42. Logozzo, S.; Zanetti, E.M.; Franceschini, G.; Kilpelä, A.; Mäkynen, A. Recent advances in dental optics—Part I: 3D intraoral scanners for restorative dentistry. *Opt. Lasers Eng.* **2014**, *54*, 203–221. [[CrossRef](#)]
43. Güth, J.-F.; Runkel, C.; Beuer, F.; Stimmelmayer, M.; Edelhoff, D.; Keul, C. Accuracy of five intraoral scanners compared to indirect digitalization. *Clin. Oral Investig.* **2017**, *21*, 1445–1455. [[CrossRef](#)] [[PubMed](#)]
44. Amin, S.; Weber, H.P.; Finkelman, M.; El Rafie, K.; Kudara, Y.; Papaspyridakos, P. Digital vs. conventional full-arch implant impressions: A comparative study. *Clin. Oral Implant. Res.* **2016**, *28*, 1360–1367. [[CrossRef](#)] [[PubMed](#)]
45. Zimmermann, M.; Mehl, A.; Mormann, W.H.; Reich, S. Intraoral scanning systems—A current overview. *Int. J. Comput. Dent.* **2015**, *18*, 101–129. [[PubMed](#)]
46. Kämpe, H.S. Studie zur Dimensionsgenauigkeit Digitaler Abformungen von Implantaten Mittels Intraoraler Scansysteme. Ph.D. Thesis, Justus Liebig University, Giessen, Germany, 2019.
47. Iturrate, M.; Eguiraun, H.; Etxaniz, O.; Solaberrieta, E. Accuracy analysis of complete-arch digital scans in edentulous arches when using an auxiliary geometric device. *J. Prosthet. Dent.* **2019**, *121*, 447–454. [[CrossRef](#)]
48. Gimenez-Gonzalez, B.; Hassan, B.; Ozcan, M.; Pradies, G. An In Vitro Study of Factors Influencing the Performance of Digital Intraoral Impressions Operating on Active Wavefront Sampling Technology with Multiple Implants in the Edentulous Maxilla. *J. Prosthodont.* **2017**, *26*, 650–655. [[CrossRef](#)]

**Disclaimer/Publisher’s Note:** The statements, opinions and data contained in all publications are solely those of the individual author(s) and contributor(s) and not of MDPI and/or the editor(s). MDPI and/or the editor(s) disclaim responsibility for any injury to people or property resulting from any ideas, methods, instructions or products referred to in the content.